LONGITUDINAL STABILITY of the BEAM BUNCH in the NSNS ACCUMULATOR RING

BNL/NSNS TECHNICAL NOTE

NO. 029

A.G. Ruggiero

May 20, 1997

ALTERNATING GRADIENT SYNCHROTRON DEPARTMENT
BROOKHAVEN NATIONAL LABORATORY
UPTON, NEW YORK 11973

Longitudinal Stability of the Beam Bunch in the NSNS Accumulator Ring

Alessandro G. Ruggiero
Brookhaven National Laboratory

May 20, 1997

Abstract

This technical note reports on the results of the investigation on the stability of the single proton bunch circulating in the NSNS Accumulator Ring against coherent longitudinal oscillations. Coherent longitudinal instabilities may be caused by the electromagnetic interaction of the beam with the surrounding. The largest contribution to the longitudinal coupling impedance are the space-charge forces. The resistive part of the longitudinal coupling impedance is a very small fraction of the total. It results that the coasting beam stability criterion, essentially determined by the space charge, sets the bunch area to a full value of 10 eV-s for the beam to be stable. Once the beam bunch dimensions, during multi-turn injection and RF compression, are blown-up to this value, no consequences to the beam stability are foreseen and the present issue does not appear to be a major concern.

The NSNS Accumulator Ring

The function of the Accumulator Ring [1] is to take the 1.0 GeV proton beam from the Linac and convert the long Linac beam pulse of about 1 ms into a 0.5 second beam in about 1100 turns. The bunch compression occurs during the injection process, and the beam is immediately extracted at the end of the process. The final beam has an intensity of 2.08×10^{14} proton per pulse, resulting in 2 MW average beam power at 60 Hz repetition rate.

The lattice of the Accumulator Ring is a simple FODO lattice with four-fold symmetry [2], and the dispersion function is reduced to zero at straight sections by the missing magnet scheme. The total circumference of the ring is 220.7 m and the transition energy is $\gamma_T = 4.93$, higher than the operating energy of 1 GeV. The salient design parameters are shown in Table 1.

The Ring Vacuum Pipe

The NSNS Accumulator Ring is made of three different sections: (i) The region of bending magnets where the shape of the vacuum pipe is rectangular with internal dimensions of 23 cm (H) and 13 cm (V). This region is expected to cover about 25 % of the whole ring circumference. (ii) The region of small quadrupoles where the vacuum pipe is circular with the internal diameter of $2b = 18$ cm. This region is expected to cover about 60 % of the ring circumference. (iii) The region of large quadrupoles where also the pipe is circular but the internal diameter is $2b = 14$ cm. This region covers the remaining 15 % of the circumference.

The analysis that follows applies strictly to circular geometry. Thus, we have approximated the rectangular vacuum chamber by a circular one with an internal diameter given by $2b = (H + V) / 2 = 18$ cm. By taking an average of the pipe dimension around the ring we have then assumed a pipe with an internal radius $b = 10$ cm. For most of the chamber components entering the analysis, it is indeed sufficient to specify a single shape and a single dimension.

Table 1: General Parameters of the NSNS Accumulator Ring

Average Power	2 MW
Kinetic Energy	1.0 GeV
Circumference, $2\pi R$	220.7 m
Bending Field	7.4 kG
Number of Protons, N	2.08×10^{14}
Betatron Tunes, $Q_{H/V}$	5.8 / 5.8
Transition Energy, γ_T	4.93
Natural Chromaticity, $\xi_{H,V}$	-6.50, -7.29
Full Betatron Emittance, ε_{tot}	120π mm mrad
Space-Charge Tune-Shift	< 0.2
RF peak Voltage (h=1)	42 kV
Revolution Frequency, f_0	1.1887 MHz
Filling Time	0.925 ms
Synchrotron Period, T_s	0.9 ms
Bunching Factor, B	0.325
Total Bunch Area, S	10 eV-s
Full Bunch Length, L	546.6 ns
Full Momentum Spread, Δ	1.6 %
Average Beam radius, a	3.80 cm
Average Pipe Radius, b	10 cm

Transverse Beam Dimension

The betatron emittance quoted in Table 1 defines the total beam, that is 100% of it. It has the same value in the two planes of oscillation. We adopted the criterion to define the total emittance ε_{tot} as 5 times the rms emittance ε_{rms}. We also define the average values of the envelope

functions $<\beta_{H,V}> = R / Q_{H,V}$, with R the average closed orbit radius and $Q_{H,V}$ the betatron tunes. The average rms beam size in the vertical and horizontal plane are then given by $\sigma_{H,V} = (<\beta_{H,V}> \varepsilon_{rms})^{1/2}$. This is the contribution from the betatron motion alone, to which we should add the contribution in the horizontal plane from the relative momentum spread δ in the beam, which is $\sigma_E = <\eta> \delta$, where $<\eta> = R / \gamma_T^2$ is the average value of the dispersion around the ring. The total beam relative momentum spread Δ is given in Table 1. The rms value δ is 1/5 of the full value.

It is sometime required to specify the average beam radius around the ring. The assumption commonly made is that the beam has a transverse uniform charge distribution and a circular shape with radius a, which we estimate to be $a = 3 [\sigma_V (\sigma_H^2 + \sigma_E^2)^{1/2}]^{1/2}$.

Low-Energy Proton Storage Rings

The frequency range and the magnitude of the wall-coupling impedance in a storage ring is determined essentially by the dimensions of the vacuum chamber and by the energy of the beam through the relativistic factor γ, the ratio of the total beam energy to the rest energy. A major feature of a low-energy storage ring is the low value of γ and therefore of the impedance frequency range of interest. In fact the cut-off harmonic number above which the beam does not interact effectively with the wall components [3] is given by $n_c \sim \gamma R/b$, where R is the average ring radius and b is the average vacuum chamber size. For a 1 GeV proton energy, a circumference $2\pi R = 220.7$ m and a vacuum chamber radius b = 10 cm, we derive $n_c \sim 726$, which is a very narrow frequency range (of only 0.61 GHz) when compared to that of high-energy storage rings (SSC, LHC, RHIC, Tevatron, ...).

The case of the NSNS Accumulator Ring is greatly simplified by the presence of a single proton bunch and by the fact that the storage ring operates well below the transition energy. Therefore results that are typical of high energy storage rings do not necessarily apply here. For instance we do not have to worry about coupled-bunch instabilities. The only modes we are concerned with are those internal to the bunch. Moreover, the beam spends only about a millisecond in the storage ring, and it is immediately extracted at the end of injection and compression. Thus, the beam has only the time to perform at most one synchrotron oscillation during the compression process. The beam can then be treated as a chopped coasting beam, and conventional coasting beam theories, when synchrotron motion is ignored, can apply.

The Longitudinal Coupling Impedance

It is customary [4] to express the beam-wall interaction by the Z/n impedance because it enters in some stability conditions. The harmonic number n is the ratio of an actual frequency to the revolution frequency. It follows strictly the definition of coasting beams. The wavelength of the charge perturbation that may cause the instability equals at most the bunch length or be less than that. Thus the range of interest is about $5 < n < 726$.

The space-charge contribution to the coupling impedance, that is the electromagnetic field stored in the region between the beam and the vacuum chamber, is the largest [5]

$$Z/n = i Z_0 (1 + 2 \ln b/a) / 2 \beta\gamma^2 \quad (1)$$

where $Z_0 = 377$ ohm and $Z/n = 150\ i$ ohm.

The next contribution is the resistivity of the wall [6]

$$Z/n = (1 - i) (Z_0 \rho_w R / 2 b^2 n)^{-1/2} \quad (2)$$

The vacuum chamber is made 85% by Aluminum and 15% by Stainless Steel. For Aluminum $\rho_w = 2.83$ μohm-cm and for Stainless Steel $\rho_w = 73$ μohm-cm. The skin depth at the revolution frequency (n = 1) is 0.39 mm for Stainless Steel and only 0.08 for Aluminum. At the lowest harmonic n = 1, we have $Z/n = (1 - i)\ 0.156$ ohm as the total contribution of both types of vacuum chamber.

Next we have contributions which are caused by discontinuity of the vacuum chamber, like bellows, strip lines, vacuum chamber steps, vacuum pump ports, and RF cavities. The detailed estimate of the contribution of all these components is given in [3]. We want to point out here that the largest contribution to the longitudinal coupling impedance, after the space-charge forces, is given by the RF cavities, followed by the vacuum ports, the vacuum chamber steps, the kicker magnet, and the bellows. The resistivity of the Aluminum vacuum chamber gives only a marginal contribution. The total longitudinal coupling impedance expected for the NSNS Accumulator Ring is plotted in Figure 1.

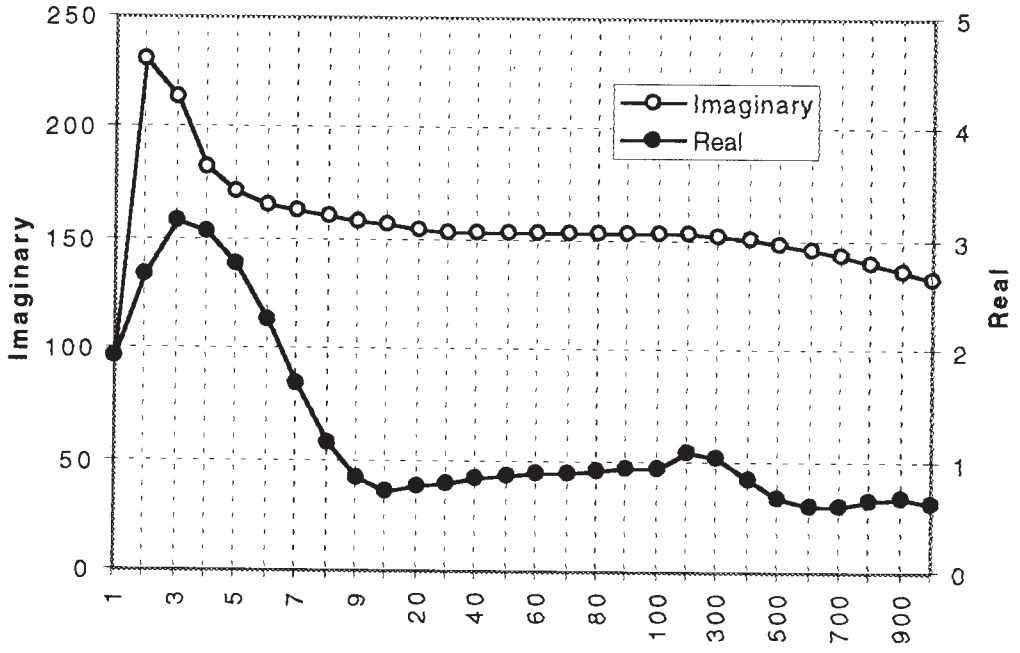

Figure 1. The Longitudinal Coupling Impedance Z/n (in ohm) vs. Harmonic Number n

Coherent Longitudinal Instabilities

There is a single long bunch. Coasting beam theory [6, 7] is first applied by estimating the complex factor

$$U' - iV' = -i\, 2\, e\, I_p\, \beta^2\, \gamma\, (Z/n) / \pi\, |\eta|\, E_0\, (\Delta E/E)_{FWHM}{}^2 \qquad (3)$$

where E_0 is the proton rest energy, β and γ are the usual relativistic factors, $(\Delta E/E)_{FWHM}$ is the FWHM value of the beam energy spread which is about half of the value of the full spread at the base, $\eta = \gamma_T{}^2 - \gamma^{-2}$, and I_p is the bunch peak current

$$I_p = Ne\, \beta c / (2\pi)^{1/2}\, \sigma, \qquad (4)$$

with σ the rms bunch length

The so-called Keil-Schnell criterion [8] seems to apply rather well for cases of accelerators and storage rings well above the transition energy when the dependence of the beam stability on the actual distribution function is not important. This is not the case well below the transition energy when it is more important to compare the actual dynamical value against the stability diagram for a give realistic distribution function.

The coasting beam form factors U′ and V′ are plotted in Figure 2 for the coupling impedance Z/n estimated for the NSNS Accumulator Ring and shown in Figure 1. It is seen that at most U′ ~ 0.9 and V′ ~ 0.012.

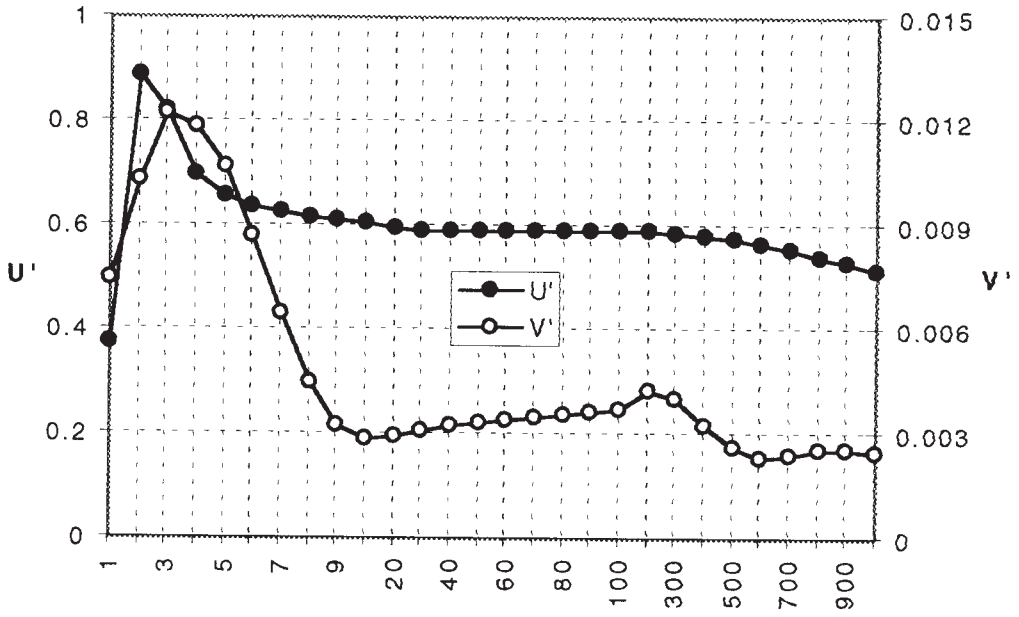

Figure 2. The Coasting Beam Form Factors U′ and V′ vs the Harmonic Number n

Taking a constant reactive impedance of -i 230 ohm as well as an exaggerated resistive contribution of 4 ohm gives U′ = 0.884 and V′ = 0.015. Figure 3 shows the stability diagram in the (U′, V′) - space for a $\cos^2$ - distribution [7]. The working point is marked with a black circle. It corresponds to a total bunch area of 10 eV-s. With this value the motion is stable. It is seen that there is plenty of safety margin for increasing, if required, the resistive contribution. Also, it is possible to include more wall components, as long they are of inductive nature so that they can subtract from the large space-charge contribution.

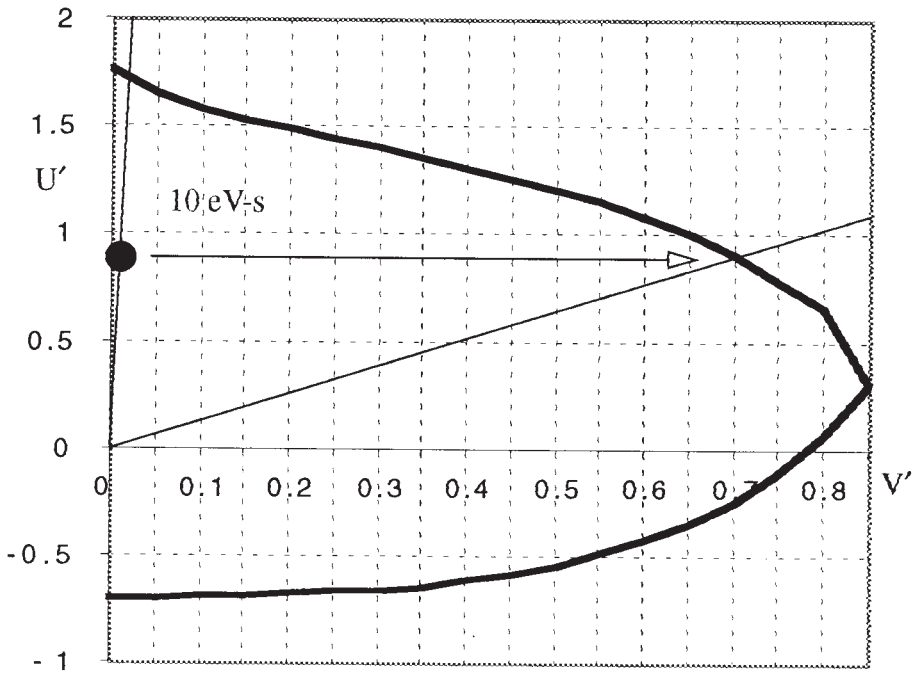

Figure 3. (U′, V′) stability diagram for $\cos^2$ - distribution

A $\cos^2$ - distribution applies well to the case the beam is compressed with a single harmonic RF system which yields a more peaked distribution. The parameters shown in Table 1 and the values given in the plots of Figures 2 and 3 correspond to this case. In reality, the strategy adopted in the NSNS Accumulator Ring [9] is to compress the beam with a dual-frequency RF system, which provides a flatter distribution and minimizes the betatron tune spread from transverse space charge forces. To represent this case, Figure 4 gives the stability diagram for a flat distribution surrounded at both sides by two half $\cos^2$ - tails, each with half the width of the flat core [7]. The working point is now by U′ = 1.06 and V′ = 0.018, a 20 % increase caused by a smaller momentum spread due to the flattening of the distribution with the same full bunch area of 10 eV-s. The shrinking of the stability region is noticeable. The case of the bunch area of 10 eV-s is outside the stability range. In order to recover stability the full bunch area is to be raised to 15 eV-s for a 2 MW beam average power, still preserving the full bunch longitudinal extension. If the beam power is 1 MW than the bunch area of 10 eV-s is still adequate for stability.

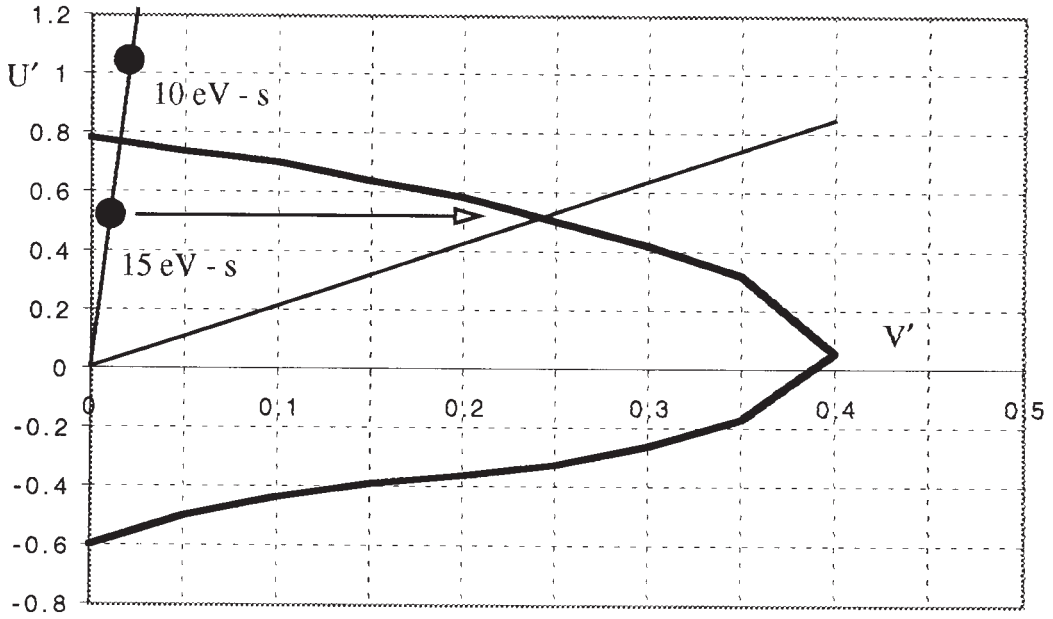

Figure 4. (U', V') stability diagram for flat-core distribution

Frequency Shifts and Growth Rates

It is convenient to calculate also two more parameters which could give further insight to the stability of the beam motion. One is the real shift of the coherent angular frequency $\Delta\Omega$ that we can calculate in absence of Landau damping, for instance, without beam momentum spread. When this quantity is normalized to the angular revolution frequency ω_0, it is given by [7]

$$\Delta\Omega / \omega_0 = (e \mid \eta \mid n I_p \, \mathrm{Im} \{Z\} / 2 \pi \beta^2 \gamma E_0)^{1/2} \tag{5}$$

The other parameter is the growth rate in absence of Landau damping given by [7]

$$1 / \tau = 0.5 \, \Delta\Omega \, \mathrm{Re} \{Z\} / \mathrm{Im} \{Z\} \tag{6}$$

It is also possible to calculate the same two quantities for a uniform distribution, which is an extreme case that is known to be unstable [6,7]. They are given by [7]

$$\Delta\Omega / \omega_0 = n \mid \eta \mid \Delta (1 + U')^{1/2} \tag{7}$$

$$1 / \tau = n \mid \eta \mid \omega_0 \Delta V' / (1 + U')^{1/2} \tag{8}$$

where the form factors U' and V' have been taken from Figure 2 after multiplying by a factor 1.4 to take into account of the reduction of the momentum spread.

The two quantities $\Delta\Omega / \omega_0$ and $1/\tau$ are plotted in Figures 5 and 6 respectively, for both momentum delta-function and uniform distribution. It is seen that both distributions give about the same range of values. Those harmonic numbers n > ~ 100 are potentially unstable with growth times equal to a fraction of the time the proton beam spends in the Accumulator Ring. To make these modes stable, it is thus imperative to provide tails of sufficient extension to the momentum distribution, and a sufficiently large bunch area as specified in the foregoing section.

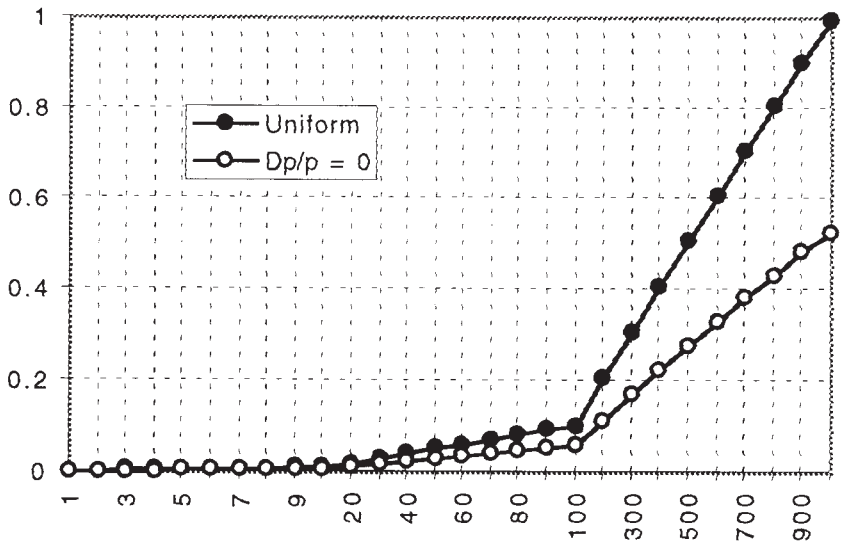

Figure 5. Frequency Shift $\Delta\Omega / \omega_0$ vs Harmonic Number n

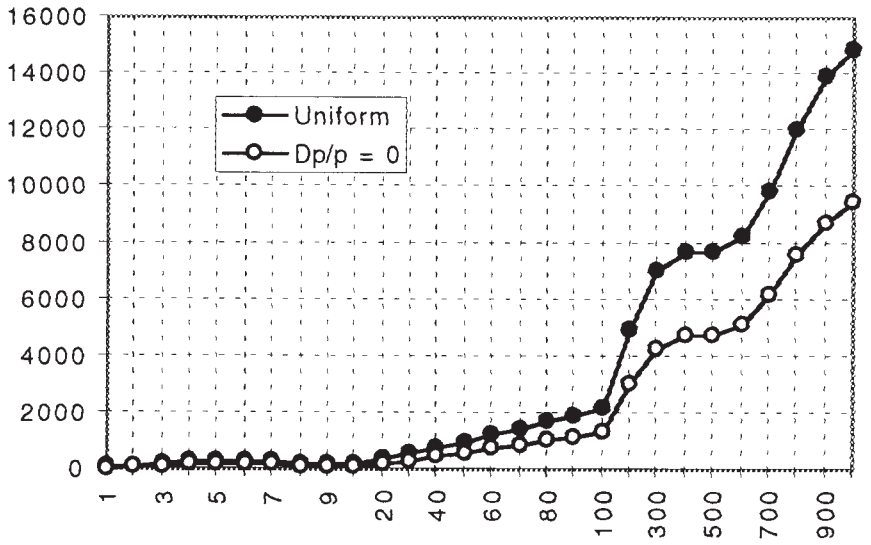

Figure 6. Growth Rate $1 / \tau$ (in s^{-1}) vs Harmonic Number n

Conclusions

It is to be mentioned that coherent longitudinal instabilities of individual bunches have never been observed in low energy proton storage rings or accelerators operating below the transition energy. This may be due to a variety of factors. First of all, since the coupling impedance is dominated by the space-charge forces contribution, which has a capacitive signature, it is difficult to introduce enough inductive wall components to alter the sign of the imaginary part of the coupling impedance. Second, only a resistive part of the coupling impedance can cause an instability. The growth rate is given by the real part of the coupling impedance, which usually is only a small fraction of the total impedance. Thus the growth rate is typically smaller than the synchrotron oscillation frequency and the coherent motion is then washed out. Of course if the beam is allowed to perform several synchrotron oscillation then one usually worries about the onset of possible head-tail instability when the transverse motion is coupled to the longitudinal motion. In the NSNS Accumulator Ring the beam performs at most one synchrotron oscillation, which thus removes also this concern.

It is important that in the NSNS Accumulator Ring the full bunch area is taken at 10 eV-s for an average beam power of 1 MW, and 15 eV-s for 2 MW, Also, in the case the beam bunch is compressed with a dual frequency RF system, the momentum distribution should be allowed to develop tails at both ends with a total width about equal to that of the flat core. When these conditions are met, it is significant the fact that the beam stability is essentially determined by the imaginary part of the coupling impedance, and that an accurate estimate of the real part is not that necessary.

References

[1] W.T. Weng et al., presentation to the 1997 Particle Accelerator Conference, Vancouver BC, May 12-16, 1997.

[2] Y.Y Lee, "The 4 Fold Symmetric Lattice for the NSNS Accumulator Ring", BNL/NSNS Technical Note No. 26, February 19, 1997.

[3] A.G. Ruggiero and M. Blaskiewicz, "Estimate of the Longitudinal Coupling Impedance for the NSNS Accumulator Ring", BNL/NSNS Technical Note No. 27, April 21, 1997.

[4] A. Sessler and V.G. Vaccaro, Internal Yellow Report, CERN 67-2, Feb. 1967.

[5] C.E. Nielsen et al., Proc. of Int. Conf. on High Energy Accel., 239, CERN 1959.

[6] V.K. Neil and A.M. Sessler, Rev. Sci. Instr. 36, 429, (1965).

[7] A.G. Ruggiero and V.G. Vaccaro, CERN - ISR - TH / 68-3, July 1968.

[8] E. Keil and W. Schnell, CERN - ISR - TH - RF / 69-48, (1969).

[9] M. Blaskiewicz, J.M. Brennan, Y.Y Lee, "RF Options for the NSNS", BNL/NSNS Technical Note No. 009, December 5, 1996.